

# MEASURING SHOCK COMPRESSION PARAMETERS IN POROUS NANOSTRUCTURED MATERIALS

Ten K.A.<sup>1\*</sup>, Prueel E.R.<sup>1</sup>, Lukyachikov L.A.<sup>1</sup>, Efremov B.P.<sup>2</sup>, Bespalov E.V.<sup>2</sup>,  
Tolochko B.P.<sup>3</sup>, Zhogin I.L.<sup>3</sup>, Zhulanov V.V.<sup>4</sup>, Shekhtman L.I.<sup>4</sup>

<sup>1</sup>LIH SB RAS, Novosibirsk, Russia, <sup>2</sup>JIHT RAS, Moscow, Russia, <sup>3</sup>ISSCM SB RAS, Novosibirsk, Russia,  
<sup>4</sup>BINP SB RAS, Novosibirsk, Russia

\*ten@hydro.nsc.ru

This article presents the results of the application of synchrotron diagnostics to study the deformation dynamics of highly-porous nanostructured SiO<sub>2</sub> aerogel under shock-wave loading.

## Introduction

Aerogels are porous materials characterized by transparency and the possibility of manufacturing in a wide range of density (0.36–0.008 g/cm<sup>3</sup>). These materials are macroscopic clusters of tightly linked silica nanoparticles. The typical size of individual particles is 3.4 nanometers. The density being low, the rigid frame takes a small fraction of the aerogel volume, i.e. almost the entire volume (up to 98–99% and more) falls on the pores. Due to the small thickness of walls, the pore dimensions do not exceed a few particle diameters.

Aerogels possess unique physical properties, including a record-low thermal conductivity combined with high transparency [1]. The speed of propagation of small perturbations in aerogels is in a power-law relation to the density and may be lower than the speed of sound in gases.

Since aerogels are subjected to high-intensity external influences, it is interesting to study their properties and behavior under dynamic and shock-wave loading. In this regard, it is necessary to indicate a number of papers on the construction of the shock adiabatic curves and equations of state of silicon aerogel [2–6].

In this study, the SiO<sub>2</sub> aerogel behavior under shock-wave loading is investigated using the features of synchrotron radiation (SR) from the accelerator VEPP-3.

## Shock-wave experiment set up

The set up of the experiments on the study of detonation and shock-wave processes is shown in Fig. 1 and described in detail in [7,8]. The shock wave in the samples was excited by a cylindrical flat piston flung by the products of detonation of explosive inside a guard ring (short-barrelled gun). Depending on its thickness and material, the piston gained velocities of 500 to 3000 m/s. We measured parameters of shock-compressed aerogel with a flat SR beam. An assembly of the sample and the loading device was placed horizontally along the plane of shaped SR beam 0.4 mm high and  $\approx$  18 mm wide. The time of the shock wave in the aerogel being within the SR beam zone was 3 to 4  $\mu$ s. During this time, we managed to make 6 to 8 snapshots (with an exposure of 1 ns) of the distribution.

This paper concerns the experimental assembly which was subjected to radical alterations. A new explosive lens was developed. A more stable plastic-

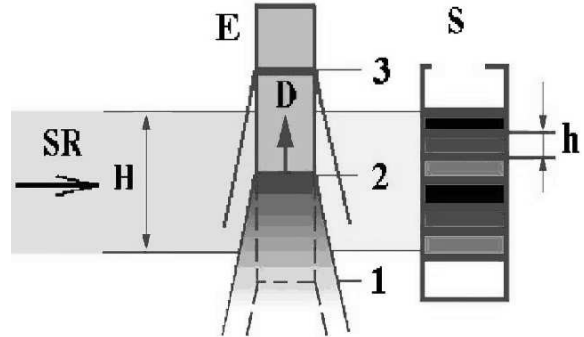


**Figure 1.** Experiment set up. SR – the flat synchrotron radiation beam, S – the DIMEX-3 detector, H – the width of the SR beam (18 mm), h – the width of detector strip (0.1 mm), E – the sample (aerogel), D – the velocity of the piston, 3 – the position of the shock front in the aerogel, 2 – the position of the piston, 1 – the border of the sample, which is deformed due to lateral unloading, or metal fragments.

based octogen explosive (with a detonation velocity of 9 km/s, VNIITF, Snezhinsk) is now used in it. The mass of the plastic explosive charge was increased up to 5 g. Parts of the new plane-wave generator are shown in Fig. 2. Fig. 3 shows a record of shock wave leaving the lens.

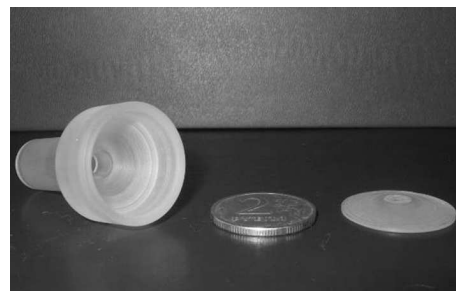


**Figure 2.** Exterior view of parts of the modified plane-wave generator.

To obtain exact interplanar distances, a new assembly made of Plexiglas was developed instead of the old (wooden) one. The new assembly allows adjusting parts with a *sliding fit* and setting distances between parts with the help of polished plates.

Due to the improvements (the new explosive lens, new explosive, and new assembly case), it is possible to conduct experiments on shock compression of aerogel at the highest possible technical level. The parallelism of the flight of the piston was verified by closure of needle sensors of 12 mm in diameter, installed along the edges of the sample, at a distance of

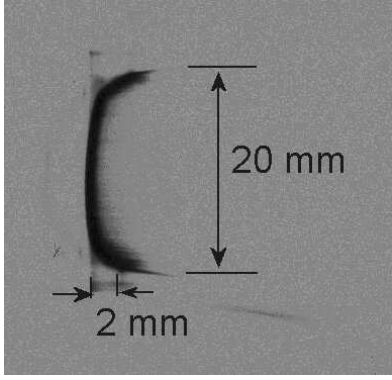


**Figure 3.** Photochronogram of shock wave leaving the explosive lens.

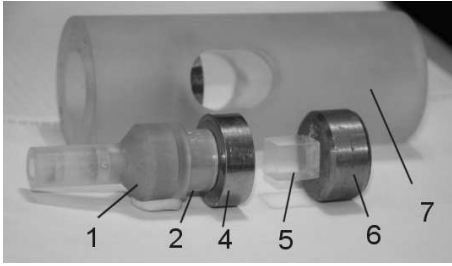


**Figure 4.** Mutual arrangement of the elements (located outside) in the assembly during the experiments on shock compression of aerogel. 1 – the explosive lens, 2 – the main HMX charge, 4 – the guard ring with the aluminum piston, 5 – the aerogel sample, 6 – the base (support), 7 – the case of the assembly.

16 mm from the gun. The oscillogram record shows a response time scatter to be less than 30 ns. The radiation was recorded with the new detector DIMEX-3 [9] which was also located in parallel to the axis of the assembly, at a distance of 980 mm from it. The recording channel dimensions were 0.4 mm in height and 0.1 mm along the axis of the charge; the total number of channels was 512. Change in the intensity of beam passing through the sample gives information about the density distribution in the measurement area.

**Results of the measurements** Fig. 5 presents the character of changes in the intensity of transmitted radiation as the shock wave is propagating in the aerogel. The experimental points were obtained in an aerogel sample of a density of  $0.25 \text{ g/cm}^3$  with an aluminum piston 3 mm thick accelerated to a speed of 1.5 km/s. It can be seen that the loading pulse front is considerably smeared, which is caused by the high porosity of the material. In each experiment, we measured the shock wave speed in target  $D$ , the mass velocity behind the wave front, which is equal to the current speed of flight of piston  $U$ , and the initial velocity of the piston. The experimental  $x-t$  diagram of the impact of the copper piston on the aerogel with a density of  $0.25 \text{ g/cm}^3$  is shown in Fig. 6.

The shock wave velocity was  $D = 1.83 \text{ km/s}$  at

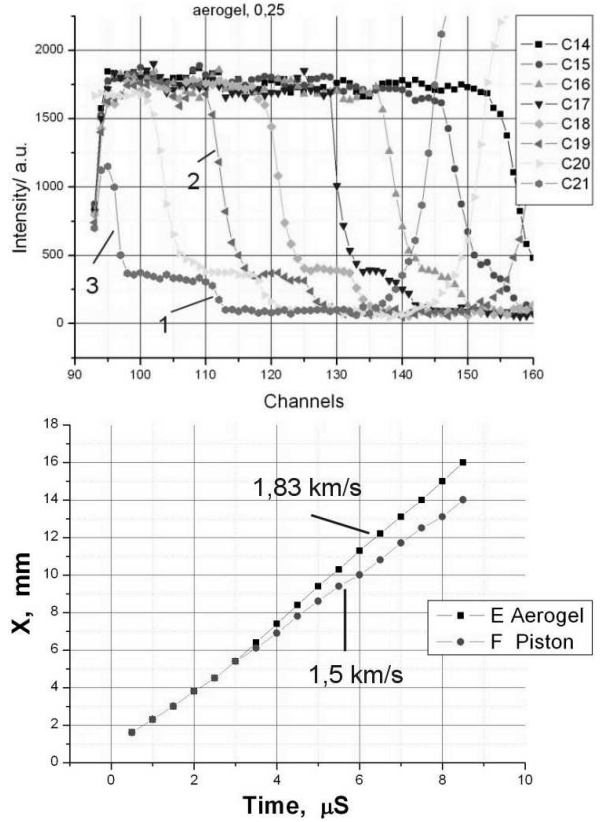


**Figure 5.** Up: dynamics of the transmitted radiation distribution. The horizontal axis is the distance expressed in the channels of the detector (1 channel is 0.1 mm). The time between frames is  $0.5 \mu\text{s}$ . 1 – the piston position, 2 – the shock front position in the aerogel, 3 – compression of the aerogel near the steel wall. Down: the piston (F) and wave front (E) coordinates obtained from the records in the left graph.

the piston velocity  $U = 1.5 \text{ km/s}$ .

Before each experiment, the DIMEX-3 detector was calibrated by measurement of transmitted radiation from aerogel plates of different thickness. This procedure allows calculating the increase in mass along the SR beam. From data in Fig. 5, the increase in mass behind the shock wave in the gel ( $m_1$ ) is  $m_1/m_0 = 5.13$ . The increase in density behind the front (at the velocities  $D = 1.83 \text{ km/s}$  and  $U = 1.5 \text{ km/s}$  in the one-dimensional approximation) is 5.54. This discrepancy may be caused by the volume expansion of the aerogel during shock compression. Since we worked with a one-dimensional detector, special experiments on the registration of lateral expansion of the aerogel were carried out. The detector was placed about a rigid wall and perpendicular to the piston motion (Fig. 6). Frame B is for the initial state of the gel; frames C, D, and E are for its state after the shock compression. After the first compression, the extension is  $\sim 6\%$ , which explains the obtained discrepancies well. After compression in the reflected wave, expansion reaches 16.6%.

The data obtained allow full determination of parameters of the compressed matter. Besides, know-

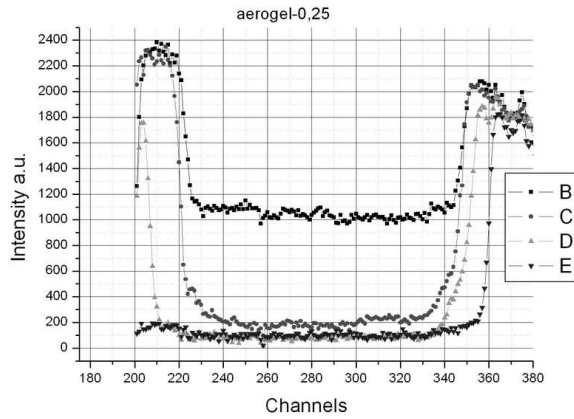


**Figure 6.** Dynamics of the distribution of transmitted radiation at the transverse detector's arrangement. The initial position of the aerogel (frame B) is between channels 222 and 344. The time between frames is  $0.5 \mu\text{s}$ .

ing the values of the initial velocity of the piston and the wave, one can calculate parameters of the aerogel compression by the deceleration method [2], because the shock adiabats of the piston material are well identified. As a result, we have determined the shock adiabats of aerogels of different initial densities, each experimental point on which was found by two methods, which improved the accuracy of the data. It should be noted that the data obtained by these methods are almost identical.

The P–U diagram of the aerogel, built for different speeds and material of the piston, is shown in Fig. 7.

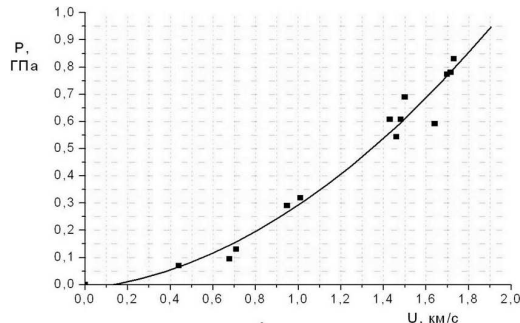


**Figure 7.** P–U diagram of the aerogel of  $0.25 \text{ g/cm}^3$ .

Our results cover the area of weak and moderate intensities of shock waves. They complement the data of [4–6], obtained at much higher intensities of shock waves.

### Conclusion

These experiments showed the feasibility of measuring aerogel compression by techniques using synchrotron radiation. A distinctive feature of our experiments is the possibility of simultaneous measurement of velocities and densities in aerogel. The results supplement the data in [2–6], obtained for high

velocities of shock compression. In the future we plan to measure compression in the reflected wave as well as increase the piston velocity up to 3–4 km/s.

This work was supported by RFBR grant No 10-08-00859 and Integration Project No 11 of SB RAS.

1. Rabie R., Dick J. J. *Equation of state and crushing dynamics of low-density silica aerogels.* // Shock compr. of Cond. Matter–1991, P. 87.
2. Demidov B. A., Efremov V. P., Ivkin M. V., Ivonin I. A., Petrov V. A., Fortov V. E. *Shock wave formation in aerogel irradiated with a high-current pulsed electron beam.* // Technical Physics. 1999. V. 69. Iss. 12. P. 18.
3. Efremov V. P., Pikuz (Jr.) S. A., Faenov A. Ya., Rozmey O., Skobelev I. Yu., Shutov A. V., Hoffmann D. H. H., Fortov V. E. *Researching the zone of energy release of heavy ion flux by methods of X-ray spectroscopy of multiply charged ions.* JETP Letters. 2005. V. 81. Iss. 8. P. 468.
4. Holmes N. C., See E. F. *Shock compression of low-density microcellular materials.* // Shock compr. of Cond. Matt., 1991. P. 91.
5. Fortov V. E., Filimonov A. S., Gryaznov V. K., Nikolaev D. N., Ternovoi V. Ya. *The generation of a non-ideal plasma by shock compression of high-porosity SiO<sub>2</sub>-aerogel.* // Modern Physics Letters A. 2003. V. 18. No. 26. P. 1835.
6. Zhernokletov M. V., Lebedeva T. S., Medvedev A. B., Mochalov M. A., Shuykin A. N., Fortov V. E. *Thermodynamic parameters and equation of state of low-density SiO<sub>2</sub> aerogel.* // Shock compr. of Cond. Matter. 2001. P. 763.
7. Merzhievsky L. A., Lukianchikov L. A., Pruel E. R., Ten K. A., Titov V. M., Tolochko B. P., Sharafutdinov M. R., Sheromov M. A. *Synchrotron diagnostics of shock-wave compression of aerogel.* // Nuclear Instruments and Methods in Physics Research, Section A. 2007. Vol. 575, Issue 1. P. 121.
8. Ten K. A., Evdokov O. V., Zhogin I. L., Zhulanov V. V., Zubkov P. I., Kulipanov G. N., Lukyanichikov L. A., Merzhievskij L. A., Pirogov B. Ya., Pruel E. R., Titov V. M., Tolochko B. P., Sheromov M. A. *Density distribution in the detonation front of cylindrical charges of small diameter.* // Combustion, Explosion and Shock Waves. 2007. No 2. V. 43. P. 91.
9. Aulchenko V. M., Baru S. E., Evdokov O. V., Leonov V. V., Papishev P. A., Porosev V. V., Savinov G. A., Sharafutdinov M. R., Shekhtman L. I., Ten K. A., Titov V. M., Tolochko B. P., Vasiljev A. V., Zhogin I. L., Zhulanov V. V. *Fast high resolution gaseous detectors for diffraction experiments and imaging at synchrotron radiation beam.* // Nuclear Inst. and Methods in Physics Research, A 623. 2010. P. 600.